

Dynamic iodide trapping by tumor cells expressing the thyroidal sodium iodide symporter

David Dingli^a, Elizabeth R. Bergert^b, Željko Bajzer^c, Michael K. O'Connor^d,
Stephen J. Russell^a, John C. Morris^{b,*}

^a Molecular Medicine Program, Mayo Clinic and Mayo Foundation, 200 First Street SW, Rochester, MN 55905, USA

^b Division of Endocrinology and Metabolism, Mayo Clinic and Mayo Foundation, 200 First Street SW, Rochester, MN 55905, USA

^c Department of Biochemistry and Molecular Biology, Mayo Clinic and Mayo Foundation, 200 First Street SW, Rochester, MN 55905, USA

^d Department of Radiology, Mayo Clinic and Mayo Foundation, 200 First Street SW, Rochester, MN 55905, USA

Received 18 September 2004

Available online 19 October 2004

Abstract

The thyroidal sodium iodide symporter (NIS) in combination with various radioactive isotopes has shown promise as a therapeutic gene in various tumor models. Therapy depends on adequate retention of the isotope in the tumor. We hypothesized that in the absence of iodide organification, isotope trapping is a dynamic process either due to slow efflux or re-uptake of the isotope by cells expressing NIS. Iodide efflux is slower in ARH-77 and K-562 cells expressing NIS compared to a thyroid cell line. Isotope retention half times varied linearly with the number of cells expressing NIS. With sufficient NIS expression, iodide efflux is a zero-order process. Efflux kinetics in the presence or absence of perchlorate also supports the hypothesis that iodide re-uptake occurs and contributes to the retention of the isotope in tumor cells. Iodide organification was insignificant. In vivo studies in tumors composed of mixed cell populations confirmed these observations.

© 2004 Elsevier Inc. All rights reserved.

Keywords: Gene therapy; Sodium iodide symporter; Isotopes; Mechanisms

The cloning of the gene for the thyroidal sodium-iodide symporter (NIS) has opened the way for the use of NIS as a therapeutic gene for cancer [1–3]. Papillary and follicular thyroid cancers have been treated for over 50 years with ¹³¹I with remarkable success, even in the presence of metastatic disease [4]. These well-differentiated tumors express NIS and concentrate ¹³¹I that decays by emission of a β particle (electron). Energy deposited by electrons within tumors generates free radicals that induce double strand breaks in DNA as well as intracellular proteins and lipids. Specific proteins within cells detect the damage and trigger either repair or apoptotic pathways [5]. Therefore, if other tumors are in-

duced to express NIS by gene transfer, they might concentrate the isotope and be destroyed by the emitted radiation. Indeed, various groups have reported that NIS in combination with radioiodine is an effective treatment strategy for prostate and breast cancer, cerebral gliomas, and multiple myeloma in animal models of disease [6–10]. However, other groups while demonstrating iodide uptake have reported only partial responses or no response at all [11–13]. This variability in responses may in part be due to differences in the intrinsic radiosensitivity of tumors, with hematopoietic tumors being the most radiosensitive.

Effective therapy with radioiodine depends not only on total isotope uptake but also on retention within the tumor cells for an adequate period of time, so that the decaying isotope can deposit sufficient energy. In

* Corresponding author. Fax: +1 507 284 5745.

E-mail address: morris.john@mayo.edu (J.C. Morris).

normal thyroid tissue, iodide undergoes a series of changes that culminate in its incorporation in tyrosine residues present in thyroglobulin, a process called “organification.” Iodide organification requires not only NIS for isotope entry into the follicular cells but additional carriers (pendrin and the apical iodide transporter) that transport iodide from within the cell to the region of the colloid (apical) as well as thyroperoxidase to oxidize iodide to iodine and conjugate it to tyrosine residues [14–16]. However, the mechanism of iodide retention in differentiated thyroid cancer (DTC) is not as clear. Various reports suggest that a substantial proportion of DTC lack the necessary machinery to organify iodide, yet therapy with ^{131}I is still effective [16,17]. Furthermore, it has been observed that tumor cells induced to express NIS leak the isotope at a relatively rapid rate [11–13,18,19]. Nonetheless, others and we have reported that NIS with ^{131}I can be effective in treating a variety of tumors in animal models [6–10]. These responses imply that the tumors are retaining the isotope.

The potential mechanisms that allow isotope retention by tumor cells to our knowledge have not been studied. We hypothesized that in the absence of organification, tumor cells that express NIS retain iodide isotopes either due to significant re-uptake of the isotope by the cells or because the limiting step is iodide efflux. Either (or both) mechanisms may result in dynamic trapping of the isotope in the tumor and thus explain the therapeutic effect. Unlike thyroid cells, tumor cells are not polarized and therefore should express NIS over all regions of their plasma membrane. *In vivo*, tumors have a three dimensional structure that places tumor cells in close proximity to each other. This geometry may allow rapid re-uptake of any isotope that leaks from one cell by surrounding cells and serve as a mechanism for isotope trapping by the tumor. In this report, we provide *in vitro* and *in vivo* evidence that these two mechanisms are active and, in part responsible for the observed therapeutic effect of NIS and radioiodine in cancer models.

Materials and methods

Cell lines. All cell lines were purchased from the American Type Culture Collection (ATCC Manassas, VA). FRTL-5 cells (Fisher rat thyroid line, ATCC# CRL-1468) were maintained in Ham's F12K medium with 2 mM L-glutamine, sodium bicarbonate (1.5 g/L) and supplemented with thyroid stimulating hormone (TSH, 10 mU/ml), insulin (0.01 mg/ml), hydrocortisone (10 nM), transferrin (0.005 mg/ml), somatostatin (10 ng/ml), glycl-L-histidyl-L-lysine acetate (10 ng/ml), and bovine calf serum (0.5%). K-562 cells (ATCC# CCL-243), a human cell line derived from a patient with chronic myeloid leukemia in blast crisis, were maintained in Iscove's modified Dulbecco's medium supplemented with fetal bovine serum (FBS, 10%), L-glutamine (4 mM), and sodium bicarbonate (1.5 g/L) [20]. ARH-77 cells (ATCC# CRL-1621), a human EBV transformed B-cell line, were maintained in RPMI 1640 supplemented with FBS (10%), glucose

(4.5 g/L), sodium bicarbonate (1.5 g/L), Hepes (10 mM), and sodium pyruvate (1 mM) [21]. All cell culture media were purchased from Gibco-BRL (Grand Island, NY). Hormones and additional growth factors were purchased from Sigma (St. Louis, MI). All cell lines were maintained at 37 °C in a humidified atmosphere with 5% CO_2 .

Generation of cell lines stably expressing NIS. K562 cells were transfected with plasmid pcDNA3-hNIS (a generous gift of SM Jhiang, Ohio State University, Columbus, OH) using the cationic lipid DMRIE-C (Gibco-BRL) according to the manufacturer's recommendations. After 3 days, the cells were expanded and then plated in limiting dilution to isolate clones by selection in geneticin (200 $\mu\text{g}/\text{ml}$). Several clones were isolated and evaluated for NIS expression by *in vitro* iodide uptake (see below). Clone EBS516 was identified due to the high iodide uptake and expanded in selection medium.

ARH-77 cells were transduced with a targeted, bicistronic lentiviral vector with hNIS and neomycin phosphotransferase under the control of immunoglobulin promoter and enhancer elements [10]. Seventy-two hours after vector transduction, the cells were placed in medium with geneticin (1 mg/ml) and the pool of surviving cells was expanded. The cells were named ARH-NIS and NIS expression was determined by *in vitro* iodide uptake as described below.

***In vitro* growth curves of cells.** ARH-77 and ARH-NIS cells were plated at a density of 2×10^5 cells/ml of medium and every 24 h an aliquot of cells from each sample was taken and counted in a hemocytometer after trypan blue staining.

***In vitro* iodide uptake studies.** Human NIS expression was tested *in vitro* by radioiodine uptake as previously described [22]. Cells were split at a density of $1 \times 10^6/\text{ml}$ and washed twice in Hanks' balanced salt solution (HBSS, Gibco-BRL). The cells were then resuspended in 0.8 or 0.9 ml HBSS supplemented with cold sodium iodide (100 μM) and buffered with Hepes (pH 7.3). One hundred microliters of potassium perchlorate (100 μM) was added to the tubes with 0.8 ml medium. Finally, 0.1 ml of sodium iodide [^{125}I] with an activity of $1 \times 10^5/0.1$ ml was added to each tube and the cells were incubated at 37 °C for 50 min. After the incubation, the cells were centrifuged at 250g for 5 min and washed twice with ice-cold HBSS. Residual activity in the cells was measured using a γ counter after a final centrifugation. All experiments were done in triplicate and untransduced cells were used as controls.

***In vitro* organification assay.** ARH-NIS and EBS516 cells were incubated as above with sodium iodide [^{125}I] for 50 min. The cells were prepared by adding 2 ml HBSS with 1% sodium dodecyl sulfate (SDS) and 50 μl of 2% sodium deoxycholate to each cell suspension followed by mixing. Intracellular proteins were precipitated by adding 1 ml of 40% trichloroacetic acid (TCA) to the lysates [23]. The samples were centrifuged for 30 min at 3300g and the supernatant was carefully aspirated. The protein precipitate was resuspended in 0.5 ml HBSS and centrifuged again under the same conditions. The supernatant was again aspirated and residual activity in the precipitate was measured using a γ counter.

***In vitro* iodide efflux studies.** We evaluated iodide efflux kinetics in cells expressing NIS as previously described by Weiss et al. [22]. Briefly, 1×10^6 FRTL-5, ARH-NIS, and EBS516 were incubated with radioiodine as described above for 50 min at 37 °C (determined by a time-course study). Efflux in FRTL-5 followed the protocol described [22]. ARH-NIS and EBS516 cells were then centrifuged rapidly on a tabletop centrifuge and the medium was aspirated. The cells were then resuspended in 1 ml cold medium (ice-cold HBSS or HBSS with potassium perchlorate, 100 μM) and incubated again at 37 °C followed by centrifugation and change of medium. This was done every 3 min and for up to 24 min. After the final incubation, the residual activity in the cells was also measured. All experiments were in triplicate. The total radioactivity present at the start of the efflux studies was back calculated by adding the activity in each sample medium with what remained in the cells at the end of the serial washes. By subtracting the activity in each timed sample from that of the total associated with the cells at time zero, the percentage of activity remaining in the cells at

that time was calculated and plotted against time. When we performed efflux experiments with the intention of maximizing iodide re-uptake, we were careful not to disturb the cell pellet to try and maintain the cells as close to each other as possible during each buffer exchange.

In vivo iodide efflux studies. Fifteen, 5-week-old female CB17 scid mice were purchased from Harlan Sprague–Dawley (Madison, WI). The mice were given levo-thyroxine in their water (5 mg/L) to suppress thyroidal NIS expression [7]. After a week of observation, the mice were given 250 cGy of total body irradiation from a ^{137}Cs source (Mark 1 Irradiation, JL Shepherd and Associates, San Fernando, CA). Twenty-four hours later they were implanted in the right flank with an equal number of washed tumor cells in 200 μl phosphate-buffered saline (PBS). Thus, five mice were injected with 1×10^7 ARH-NIS cells (100% NIS expression), five mice with 5×10^6 ARH-NIS and 5×10^6 ARH-77 cells (50% NIS expression), and five mice with 1×10^6 ARH-NIS and 9×10^6 ARH-77 (10% NIS expression). Tumor growth was monitored and when the mean tumor diameter was 0.6 cm, three mice from each group were injected with ^{123}I (18.5 MBq intraperitoneally, ip). The mice were imaged serially with a γ camera (Helix System, Elscint, Haifa, Israel) at 1, 3, 5, and 6 h after isotope injection.

Using region of interest analysis, the total counts in each mouse and in the corresponding tumor were determined. The counts were corrected for γ camera background activity and for decay of ^{123}I (half-life = 13.2 h). Total activity in each mouse and in each tumor was expressed as a percentage of total body activity in the 1-h image.

All studies involving animals were approved by the Institutional Animal Care and Use Committee (IACUC) and performed according to AAALAC approved procedures.

Statistical analyses. All statistical testing was done using StatView software (SAS Institute, Cary, NC). Spearman's rho was used for correlation analysis and Wilcoxon's rank sum test was used to compare means with a $p < 0.05$ taken as the value for significance. All curve fitting was performed using KaleidaGraph (Synergy Software, Reading, PA).

Results

Cells transduced with vectors coding for NIS concentrate radioiodine

We developed two suspension cell lines that express human NIS: ARH-NIS (from ARH-77) and EBS516 (from K-562) as described in Materials and methods. The cells were expanded under selection with geneticin and tested for NIS expression by an in vitro iodide uptake assay as described previously [22]. Both cell lines expressed NIS and concentrated iodide (Fig. 1). Iodide uptake was significantly decreased but not eliminated by potassium perchlorate, a specific inhibitor of NIS. Assuming that the cells are spheres with a mean diameter of 10 μm , we estimated that the intracellular iodide concentration was almost 100-fold higher relative to the extracellular medium. This compares favorably with thyroid cells that normally concentrate iodine between 20- and 40-fold compared to the extracellular fluid concentration. Since we used the same number of cells for the uptake studies, it appears that the EBS516 cells express higher levels of NIS leading to a higher uptake of isotope.

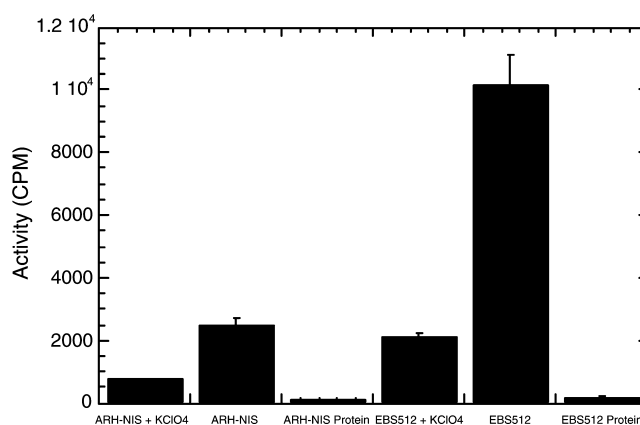


Fig. 1. ARH-NIS and EBS516 cells express NIS and concentrate radioiodine [^{125}I]. Iodide uptake is specifically inhibited by perchlorate that competes with iodide for binding to NIS. The bars represent the mean of triplicate experiments. The cells do not incorporate iodide into protein to any significant extent (<3% of total activity appeared in the protein precipitate).

Cell lines expressing NIS release iodide slower than thyroid cells

We wanted to evaluate the efflux kinetics of iodide in the two cell lines and compare it to that of thyroid cells. In this experiment, FRTL-5 cells were used as controls. The experimental design is described in the Materials and methods. Central to our hypothesis is the geometry of the tumor that may allow tumor cells to reabsorb any isotope that may leak out. Thus, unless otherwise stated, in all efflux experiments we were careful not to disturb the cell pellet during each exchange of media to mimic as closely as possible the scenario in vivo. Iodide efflux was very rapid in FRTL-5 cells and significantly slower in both tumor cell lines tested (Fig. 2). The efflux half time (the time taken for the intracellular activity to fall

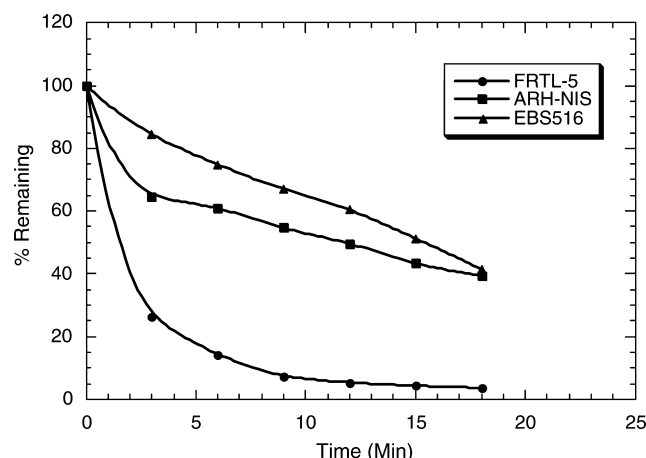


Fig. 2. Iodide efflux is slower in tumor cells compared to a rat thyroid cell line (FRTL-5). Efflux studies were performed as described by Weiss et al. [17]. Each time point is a mean of three independent observations.

to 50%) was 2 min in the case of FRTL-5, 12.5 min for ARH-NIS, and 20 min for EBS516. Fig. 2 also shows that in both EBS516 and ARH-NIS cells, remaining activity decreases almost linearly with time, suggesting that in these cells efflux is independent of intracellular iodide concentration (a zero-order process). We have mathematically modeled iodide efflux in these cells (see Appendix) and found that the assumption of zero-order rate of efflux is more compatible with the experimental data than the assumption of first-order rate. With FRTL-5 cells, there is a rapid initial loss of activity and then a slower decline compatible with a first order process, i.e., exponential decay. This can be explained, in part, by the presence and number of passive iodide transporters pendrin and the apical iodide transporter (AIT) [14,15]. These proteins are not known to be expressed on hemopoietic cells but iodide still leaks from tumor cells. The absence of these two proteins can explain some of the difference in iodide efflux, although potential iodide leak through other membrane anion transporters as well as quantitative differences in the levels of pendrin and AIT cannot be excluded. Iodide binds non-specifically and is trapped between cells, even in the absence of NIS. This non-specific trapping, amounting to about 300 cpm for ARH-NIS and 600 cpm for EBS516, is lost with the first buffer exchange and explains the initial rapid loss from ARH-NIS cells that concentrate the isotope to a lesser extent than EBS516 (see Figs. 1 and 3). Our data are similar to those of Nakamoto et al. [24] who demonstrated that iodide efflux is significantly slower in MCF7 breast carcinoma cells induced to express NIS compared to FRTL-5.

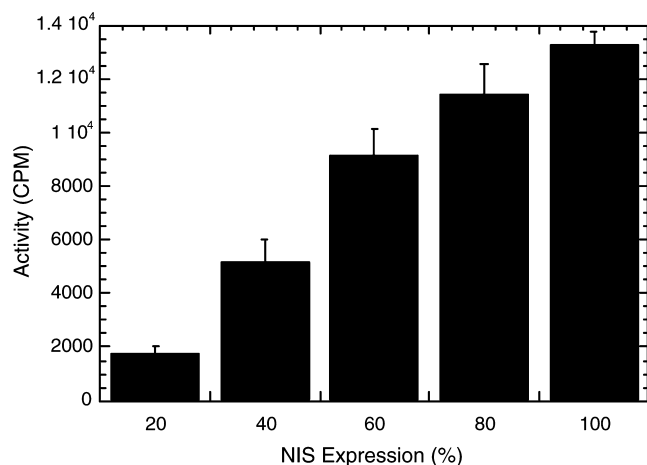


Fig. 3. Radioiodine uptake increases linearly with the number of cells expressing NIS. In vitro iodide uptake was performed in EBS516 and ARH-NIS cells by varying the proportion of cells expressing NIS but keeping the total cell population constant. The data shown are for EBS516. Similar results were obtained with ARH-NIS.

Iodide organification does not explain the difference in efflux kinetics

The incorporation of iodide with intracellular protein (organification) might explain the difference in iodide efflux observed. Thus, we tested our cell lines for their ability to organify iodide. After a 50-min incubation with ^{125}I , cells were lysed and proteins were precipitated using trichloroacetic acid [23]. Residual activity in the precipitate was measured after a final wash with cold buffer. As can be seen from Fig. 1, there was very little iodide associated with the protein precipitate (less than 3% of the total intracellular activity). Thus, the two cell lines do not incorporate iodide into protein and some other mechanism must explain the longer iodide retention time in these cells. We reasoned that two potential mechanisms to explain this discrepancy might be either that iodide efflux from these cells is limiting or that there is significant isotope re-uptake by the cells.

Iodide efflux and NIS expression

If tumor cells behaved as independent units, then isotope uptake in cells should vary linearly with the number of cells expressing NIS. We tested this possibility by performing in vitro iodide uptake studies with different numbers of cells expressing NIS but keeping the total number of cells in the incubation constant at 1×10^6 . The proportion of cells expressing NIS varied from 20% to 100%. After incubating the cells with isotope for 50 min, the cells were pulsed in a microcentrifuge, the supernatant was carefully aspirated, and the activity in the cell pellet was measured. As the number of cells increased, the activity present in the cells at the end of the incubation increased linearly with the proportion of cells expressing NIS (Fig. 3).

The linear efflux kinetics in tumor cells expressing NIS implies that the efflux pathway is rate limiting. We reasoned that performing efflux experiments with mixed populations of cells, some expressing NIS and some not, could shed light on the problem. In a series of five experiments, EBS516 and K-562 were mixed so that the proportion of cells expressing NIS varied from 20% to 100% (in 20% increments). After a 50-min incubation with ^{125}I , the cells were incubated with cold buffer as described in the methods section. Remaining activity decreased linearly with time and iodide efflux follows zero-order kinetics, i.e., it is independent of iodide concentration (Figs. 4A–F). The slopes of the curves decreased as the number of cells expressing NIS increased, implying that net isotope efflux is slower. The only exception is Fig. 4A where the slope of the curve is lowest (−2.18) whereas one would expect it to be the highest. The reasons behind this discrepancy are unclear. However, radioiodine binds non-specifically to cells even if they do not express NIS and some activity

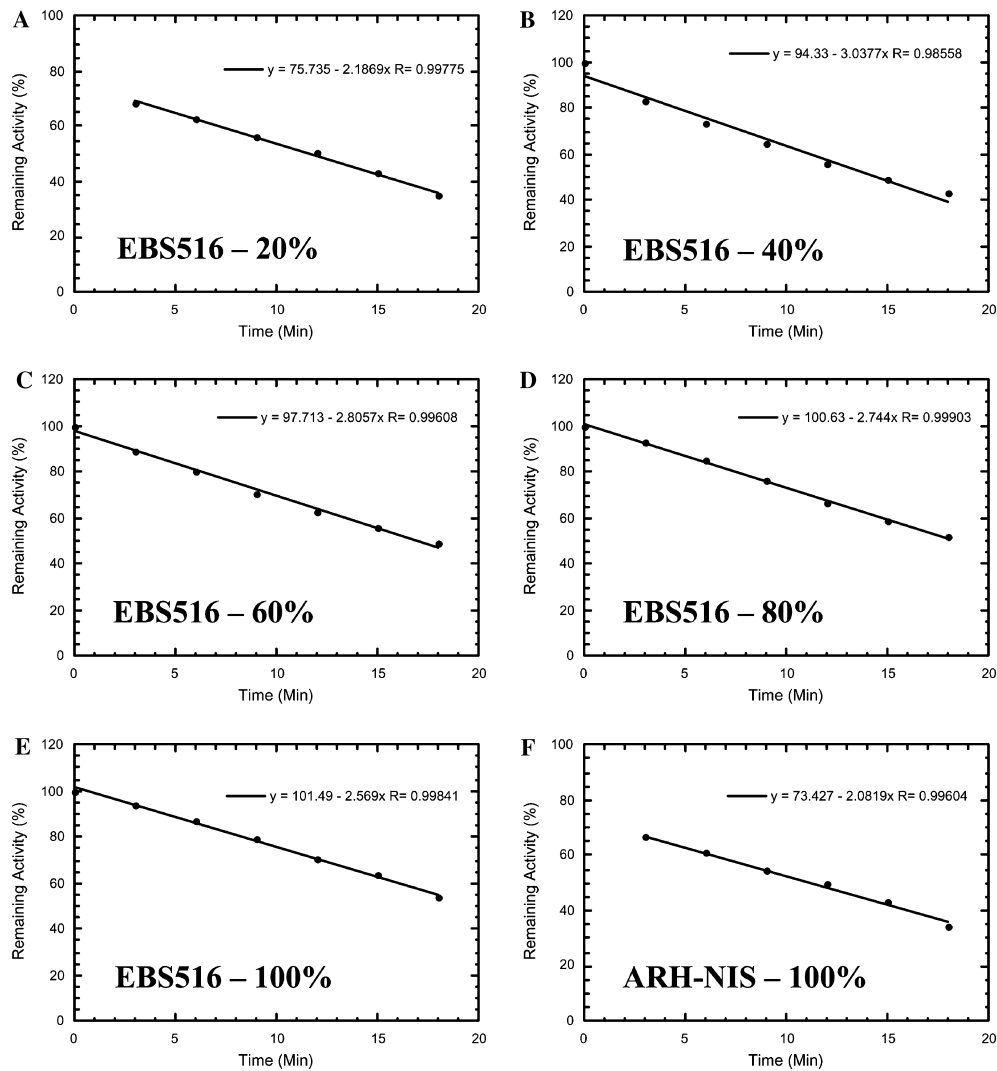


Fig. 4. The number of cells expressing NIS determines iodide efflux kinetics. The experimental design is described in Materials and methods. Iodide efflux rates decrease as the number of cells expressing NIS increases, supporting the hypothesis that re-uptake is important. (A–E) EBS516 cells with (A) 20%, (B) 40%, (C) 60%, (D) 80%, and (E) 100% cells expressing NIS. (F) Representative example from similar experiments with ARH-NIS cells.

is also trapped in the buffer present in the cell pellet. This activity is usually low and insignificant when iodide uptake is very high. However, when iodide uptake is sufficiently low, it introduces a significant error. Indeed, the y -intercept for Fig. 4A is 75.7 when it should be 100. We observed the same phenomenon with ARH-NIS cells that concentrate the isotope to a lower extent than EBS516 (Fig. 4F). The curves also move to the left as the proportion of cells expressing NIS decreases and the retention half time falls. We calculated the retention half time for each cell line under each condition and observed that half time is closely related both to the proportion of cells expressing NIS as well as peak iodide uptake at the end of the incubation (Fig. 5 and data not shown). These results suggest that efflux is not only zero order but also that initial iodide uptake (a surrogate for NIS expression) plays a determining role in isotope retention that is best explained by re-uptake. A

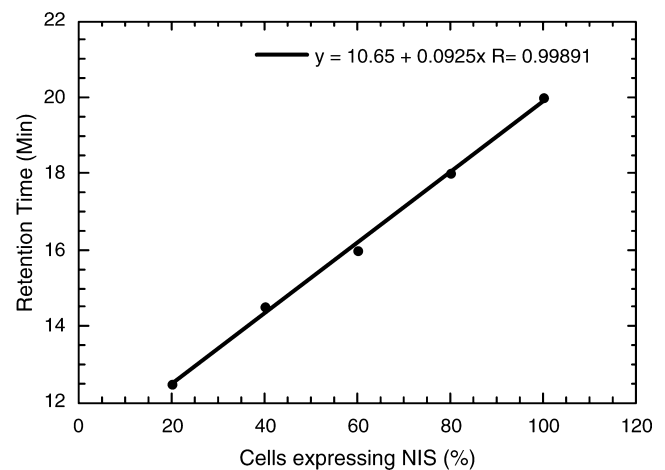


Fig. 5. Iodide retention half time is directly proportional to the number of cells expressing NIS. The data shown are for EBS516. Each time point is a mean of three observations. $R = 0.99$. Similar results were obtained with ARH-NIS.

mathematical model of this behavior is presented in the Appendix where we demonstrate that the slope for iodide efflux is linearly dependent on the inverse of the initial iodide uptake (Fig. 9).

Thus, it appears that if cells concentrate iodide above a certain threshold, efflux is determined by the availability of the carrier mechanism responsible for the iodide leakage. As a corollary, to maximize the therapeutic effect of NIS, high level transduction and expression are required.

Iodide re-uptake and retention

While carrier mediated efflux may be limiting at high concentrations, this mechanism does not exclude the possibility of iodide re-uptake by cells expressing NIS. If cells behaved as individual units, efflux kinetics should be the same and the curves parallel to each other, irrespective of the number of cells expressing NIS. The fact that the slopes of the efflux curves (Fig. 4) decrease as the number of cells expressing NIS increases suggests that iodide re-uptake may be contributing to isotope retention in these cells. To evaluate further the potential role of tumor geometry in isotope retention, we performed parallel efflux experiments with cells either in suspension or maintained as a pellet. Keeping cells in suspension should limit iodide reuptake by decreasing the effective concentration of the leaked isotope around the cells. As can be seen from Fig. 6A, iodide efflux is significantly slower when the cells are maintained as a pellet compared to when they are re-suspended in the medium (slopes -0.81 and -1.82 , respectively). This suggests that if cells expressing NIS are close to each other, they can reabsorb iodide that leaks out from surrounding tumor cells.

To further explore this hypothesis, we performed parallel iodide efflux studies where the cells were repeatedly incubated with Hanks' balanced salt solution (HBSS) with or without potassium perchlorate ($100\ \mu\text{M}$). Perchlorate in the medium competes with iodide for binding to NIS and limits reuptake of the isotope. As can be seen from Figs. 6B and C, perchlorate increased the rate of iodide efflux from cells (slopes increase in value), irrespective of the proportion of cells expressing NIS. We conclude that isotope re-uptake is an important mechanism for iodide retention by cells expressing NIS and that the relative position of cells expressing NIS in the tumor may play an important role in isotope trapping.

In vivo isotope retention by tumor xenografts expressing NIS

The data above suggest that tumors with a higher number of cells expressing NIS should retain iodide longer due to isotope re-uptake. To evaluate this possibility in vivo, we established mixed myeloma (ARH-77

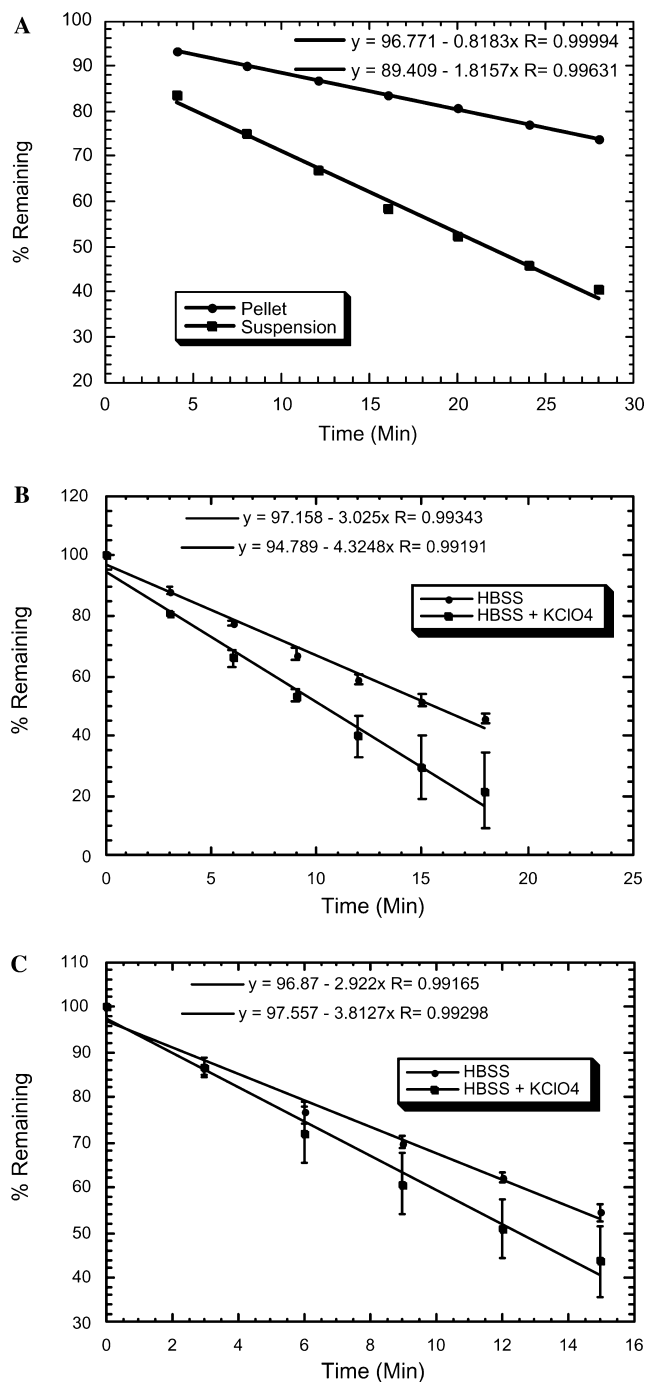


Fig. 6. (A) Geometry influences the rate of iodide release from the tumor. Iodide efflux experiments were performed in parallel in EBS516 cells maintained as a pellet or as a suspension after equilibration with ^{125}I . Iodide efflux is slower in the cell maintained as a pellet compared to the cell in suspension. (B,C) NIS-mediated iodide re-uptake contributes to dynamic trapping of the isotope in tumor cells. Iodide efflux kinetics were determined for ARH-NIS (B) and EBS516 (C) in the presence and absence of perchlorate. KClO_4 leads to an increase in the net rate of iodide efflux from tumor cells expressing NIS. All experiments were performed in triplicate.

and ARH-NIS) tumors in SCID mice. An important assumption in this experiment is that the proportion of ARH-77 and ARH-NIS cells in the growing tumors

remains similar to the ratio of injected cells. This requires that the two cell lines grow at similar rates. We evaluated the growth rate of the two cell lines in vitro and as can be seen from Fig. 7A, their growth rates

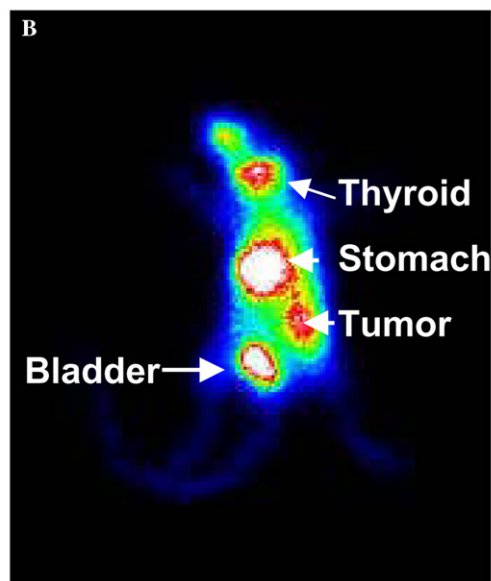
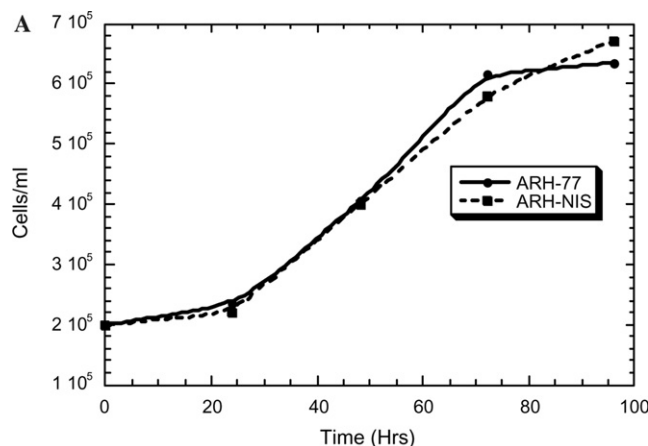


Fig. 7. (A) ARH-77 and ARH-NIS cells grow at almost identical rates in culture. (Wilcoxon, $p = 0.584$). (B) γ camera scintiscan of a SCID mouse bearing a tumor xenograft with only 10% of the cells expressing NIS. The tumor can be clearly visualized in the right flank using a γ camera after ^{123}I injection. The image is taken 1 h after isotope injection and the exposure time was 5 min.

are virtually identical. Thus, we proceeded to implant mixed tumors in SCID mice where 10%, 50% or 100% of the cells expressed NIS. All the mice were injected with the same total number of cells that were grown under identical conditions. Tumor xenografts developed in all mice and grew at similar rates (not shown). When the tumors reached a mean diameter of 0.6 cm, the mice were injected intraperitoneally (ip) with ^{123}I (a γ ray emitting isotope) and imaged serially starting 1 h after isotope injection. All the tumors concentrated ^{123}I and could be clearly visualized using a γ camera. A representative example from a mouse with a tumor having only 10% of the cells expressing NIS is presented in Fig. 7B.

We calculated how intratumoral isotope activity changed with time after correction for the physical half-life of the isotope. As can be seen from Figs. 8A–C, isotope retention time increased as the proportion of cells expressing NIS increased from 2.8 h when only 10% of the tumor cells expressed NIS [C] to 5.4 h when all the cells expressed the symporter [A]. The slopes of the three curves also increased as the number of cells expressing NIS decreased (-8.99 [A] > -11.34 [B] > -15.7 [C]), showing that net isotope loss is faster as the number of tumor cells expressing NIS decreases.

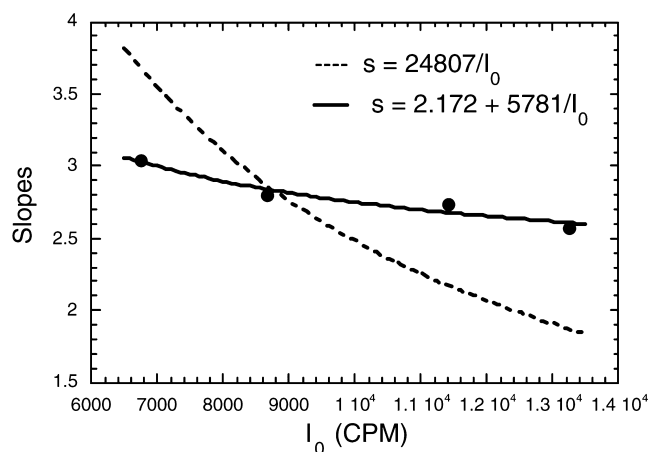


Fig. 9. The rate of iodide efflux is dependent on peak isotope uptake, I_0 . Slopes from Fig. 4 were plotted against peak iodide uptake for the same cells. In our model the best-fit function for slopes implies a linear relationship between D of Eq. (A.6) and I_0 .

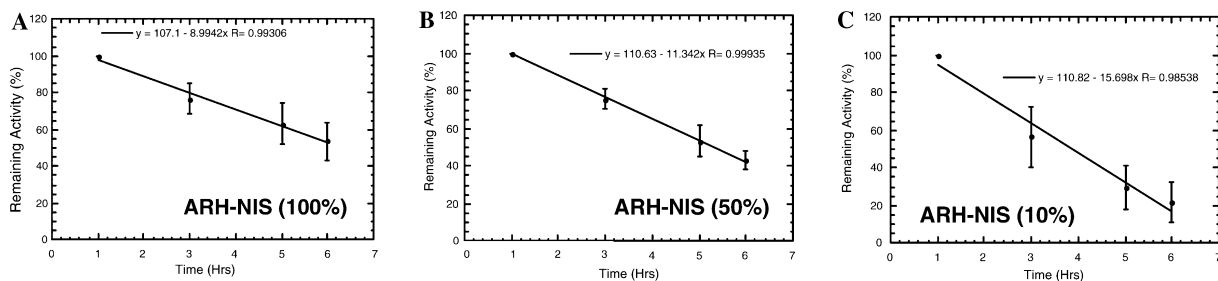


Fig. 8. In vivo iodide retention by tumor xenografts depends on the number of cells expressing NIS. Myeloma tumor xenografts were established in SCID mice, such that 100% (A), 50% (B) or 10% (C) of the cells expressed NIS.

As reported elsewhere, longer retention time was translated into a therapeutic effect using ^{131}I (37 MBq); tumors where 50% or 100% of the cells expressed NIS regressed while tumors with only 10% of the cells expressing NIS were transiently slowed but ultimately continued to grow [25]. These results highlight the importance of isotope retention in tumors for iodine to have a significant impact on tumor growth.

Discussion

The cDNAs for rat and human NIS were both cloned in 1996 [1,2]. Since then, the biochemistry of NIS and its interaction with various anions have been well studied. NIS transports one iodide ion with two sodium ions, the process being driven by the low sodium ion concentration in cells [26,27]. Ion binding is non-random; two sodium ions are bound first followed by an iodide ion. The three ions are then translocated across the plasma membrane of cells [26]. Apart from enhancing our understanding of iodide physiology in the thyroid, the availability of the cloned gene opened the way for its use as a therapeutic and/or reporter gene in cancer therapy. The therapeutic efficacy of NIS with ^{131}I in animal models of cancer is well established [6–10]. However, other investigators have reported that there is no therapeutic effect from the combination of NIS with ^{131}I due to rapid isotope efflux from the tumor [11–13]. In addition, NIS has been used as a reporter gene to track the in vivo distribution of vectors injected in animal models [9,28,29]. NIS is a very versatile protein that can concentrate various isotopes with different physical characteristics allowing tailored therapy for different tumors [26,27,30]. Iodide isotopes allow γ camera or positron emission tomography imaging while various other anions taken up by NIS such as ^{131}I , ^{188}Re , and ^{211}At emit either β or α particles that can have a therapeutic effect on cancer cells.

Thus, NIS is now established as an important molecule in the field of cancer gene therapy. Although there are still concerns regarding its efficacy in animal models, the mechanisms of its effect have not been studied. Specifically, the reason(s) behind iodide (and other anion) retention in tumors, a feature that is key to its success in tumor therapy, have not been evaluated. In this report, we shed some light on the potential mechanisms underlying iodide trapping in these cells. We demonstrate that iodide uptake in these two tumor cell lines is dependent on the concentration of NIS in the cells and that tumor cell lines expressing NIS leak out the isotope at a rate that is slower than thyroid cells. Thyrocytes leak iodide rapidly due to the presence of passive iodide transporters on the apical surface of these cells. Two such transporters have been identified so far: pendrin and the AIT [14,15]. Theoretically, NIS can serve

as a reverse carrier of iodide from inside to the outside of the cell, but the high sodium ion concentration outside the cell should effectively eliminate this possibility. In tumor cells expressing NIS, efflux kinetics depends on the level of NIS expression. Cells that express high amounts of NIS concentrate iodide such that efflux is determined by the availability of the carrier mechanism responsible for the iodide leak. In addition, NIS can take up anions that have leaked from the cell again (re-uptake). Thus, aiming for high level expression of NIS makes sense not only for maximal iodide uptake but also to ensure adequate retention if the isotope is to have its desired effect.

Our in vitro experiments were designed to take into consideration geometrical factors that can influence therapy with iodide isotopes in an in vivo system. Our hypothesis was that having tumor cells expressing NIS in close proximity might allow rapid isotope re-uptake similar to what could happen in vivo. Thus, we were careful not to disturb the cell pellet during the repeated buffer exchanges performed for the efflux studies in an attempt to mimic as closely as possible the local environment in the tumor. Gentle buffer exchanges may simulate the tumor microcirculation that washes out some of the leaked iodide and limits isotope re-uptake. Our in vitro data suggest that tumor cells related to each other in space retain radioiodine by a combination of slow efflux and re-uptake. While slow efflux is a property of an individual cell and dependent on the availability of the efflux proteins, efficient re-uptake is a property of the tumor that is probably dictated by its geometry. Close proximity of cells expressing NIS maximizes re-uptake and trapping of the isotope. The importance of geometry is further highlighted by comparing our efflux studies with those where adherent cell monolayers are used [12,13,18,19]. Isotope retention times for cells maintained as monolayers are shorter compared to those of our cell lines, since the probability of isotope re-uptake is smaller in a monolayer. The in vivo data with tumors having mixed cell populations support our hypothesis; isotope retention time depends on the percentage of cells expressing NIS.

Tumor geometry is an additional consideration in the choice of isotope used for therapy. β particle emitters are attractive therapeutic isotopes because the emitted electrons have a variable path length that ranges from the sub-micrometer to more than a centimeter [31]. The macroscopic path length of emitted electrons has the potential of a bystander effect; tumor cells that do not express NIS can still be destroyed by electrons emitted from surrounding transduced tumor cells that express NIS and concentrate the isotope. Indeed, we have shown that such a bystander effect from ^{131}I exists (median electron path length = 0.4 mm, range 0.04–2.4 mm) [10,31]. Thus both tumor geometry and the distribution of NIS expressing cells within the

tumor can influence the success of therapy by maximizing particle crossfire. Any local anisotropy in NIS expression might decrease the effectiveness of therapy. The tumor microcirculation might play an important role by influencing the local delivery of systemically administered vectors as well as washing away any leaked isotope. While our studies did not take these issues into consideration, it is noteworthy that in vivo, the number of cells expressing NIS still determined isotope retention time and ultimately the response of the tumors to ^{131}I .

It has been suggested that the cytoreductive effect of NIS with radioiodine can be enhanced by the simultaneous expression of thyroperoxidase for iodide organification that might prolong isotope retention in tumors [32]. Interestingly, in that report, thyroperoxidase expression did not have any influence on retention half-time, even though total isotope activity in cells increased. While it is possible to design vectors with two therapeutic genes, one has to consider the possible decrease in titer yield as vector genome length increases. A lower vector titer might decrease the number of transduced cells and therefore potentially decrease the overall therapeutic effect of radioiodine. Finally, other anion transporters might be responsible for iodide efflux from cells. Thus, investigators have attempted to reduce the rate of isotope efflux from cells expressing NIS using anion transporter inhibitors or lithium but without any benefit [12,13,19].

In conclusion, we show that tumor cell lines expressing NIS retain iodide longer than thyroid cells due to a combination of slow efflux and re-uptake. Iodide organification does not contribute significantly to isotope retention. Intratumoral isotope retention time is determined by the concentration of NIS in the local microenvironment. A dynamic mechanism explains isotope trapping in tumor cells expressing NIS.

Acknowledgments

We thank Dr. S.M. Jhiang, Ohio State University, Columbus, Ohio, for the NIS cDNA (pcDNA3-hNIS), Mary E. Harvey and Royce Ruter for excellent technical assistance with the animal experiments. This work is supported by Grants CA 83181 to S.J.R. and CA 91956 to J.C.M.

Appendix A

A simple kinetic model can be established to quantitatively describe iodide efflux as presented in Figs. 4A–F. The change of iodide concentration in cells $I(t)$ is assumed to obey zero-order kinetics in efflux with the rate r . Iodide reflux (re-uptake) is established as a second or-

der process depending both on iodide concentration $I_e(t)$ in the extracellular space and on NIS concentration, N , considered constant during the experiment. $I_e(t)$ is initially zero. Thus, before the first washout at time t_1 , one has

$$\begin{aligned} I'(t) &= -r + kNI_e(t), \quad I(0) = I_0 \\ &= I(t) + I_e(t), \quad 0 \leq t \leq t_1, \end{aligned} \quad (\text{A.1})$$

where k is the rate constant for reflux. Clearly, there is conservation of iodide in the system: it is either in the cells or in the extracellular space. The above system of equations yields one linear differential equation

$$I'(t) = -r + kN[I_0 - I(t)], \quad I(0) = I_0, \quad 0 \leq t \leq t_1. \quad (\text{A.2})$$

After the first wash-out, i.e., for $t > t_1$, the intra-cellular $I(t)$ is governed by the analogous equation

$$I'(t) = -r + kN[I_1 - I(t)], \quad I_1 = I(t_1), \quad t_1 \leq t \leq t_2, \quad (\text{A.3})$$

where, of course, $I(t_1)$ is given by Eq. (A.2), and it reflects the starting intracellular concentration after the washout, while it is assumed that initially there is no extracellular iodide left. In general, after the n th wash-out

$$\begin{aligned} I'(t) &= -r + kN[I_n - I(t)], \quad I_n = I(t_n) \\ t_n \leq t \leq t_{n+1}, \quad n = 0, 1, \dots, \quad t_0 > 0. \end{aligned} \quad (\text{A.4})$$

The solution of this initial value problem is obtained by using standard methods for solution of linear differential equation and can be written as

$$I(t) = I_n + r(e^{-kN(t-t_n)} - 1)/kN, \quad t_n \leq t \leq t_{n+1}. \quad (\text{A.5})$$

This equation when specified for $t = t_{n+1}$ leads to the following iterative formula for concentration I_n :

$$\begin{aligned} I_{n+1} &= I_n - D, \quad D = \frac{r}{kN}(1 - e^{-kN\Delta t}), \\ \Delta t &= t_{n+1} - t_n, \quad n = 0, 1, \dots, \end{aligned} \quad (\text{A.6})$$

where we assumed equal time intervals Δt between any two washouts, as it was chosen in the experiment ($\Delta t = 3$ min). Formula (A.6) indeed predicts the linear decrease of I_n observed in Fig. 4

$$I_n = I_0 - nD, \quad n = 0, 1, \dots \quad (\text{A.7})$$

The quantity I_n/I_0 is actually plotted in Fig. 4, implying that the slope $s = D/I_0$ would depend on the initial concentration I_0 unless D is proportional to I_0 . The slopes s estimated from Figs. 4B–E do show some dependence on I_0 (Fig. 9), but this is not consistent with $1/I_0$ decrease, but rather, it is well fitted by the function $s = a + b/I_0$. This implies that $D = I_0s = aI_0 + b$. Dependence of D on I_0 can be understood as a consequence of Eq. (A.6) in which D depends on NIS concentration that

in turn determines I_0 . One can assume that $I_0 = f(N)$ where f is certain invertible function and, then $N = f^{-1}(I_0)$, so that D is certain function of I_0 . According to the fit in Fig. 9, this function may be well approximated by the linear function.

It should be noted that if one would assume that efflux rate depends on the instant intracellular iodide concentration, i.e., $r = k_e I(t)$, the resulting model would not yield observed linear decrease of I_n but show behavior according to $I_n = I_0 q^n$.

References

- [1] G. Dai, O. Levy, N. Carrasco, *Nature* 379 (1996) 458–460.
- [2] P.A. Smanik, Q. Liu, T.L. Furminger, K. Ryu, S. Xing, E.L. Mazzaferri, S.M. Jhiang, *Biochem. Biophys. Res. Commun.* 226 (1996) 339–345.
- [3] L.A. Pinke, D.S. Dean, E.R. Bergert, C. Spitzweg, C.M. Dutton, J.C. Morris, *Thyroid* 11 (2001) 935–939.
- [4] E.L. Mazzaferri, R.T. Kloos, *J. Clin. Endocrinol. Metab.* 86 (2001) 1447–1463.
- [5] R.T. Abraham, *Genes Dev.* 15 (2001) 2177–2196.
- [6] C. Spitzweg, S. Zhang, E.R. Bergert, M.R. Castro, B. McIver, A.E. Heufelder, D.J. Tindall, C.Y. Young, J.C. Morris, *Cancer Res.* 59 (1999) 2136–2141.
- [7] C. Spitzweg, M.K. O'Connor, E.R. Bergert, D.J. Tindall, C.Y. Young, J.C. Morris, *Cancer Res.* 60 (2000) 6526–6530.
- [8] U.H. Tazebay, I.L. Wapnir, O. Levy, O. Dohan, L.S. Zuckier, Q.H. Zhao, H.F. Deng, P.S. Amenta, S. Fineberg, R.G. Pestell, N. Carrasco, *Nat. Med.* 6 (2000) 871–878.
- [9] J.Y. Cho, D.H. Shen, W. Yang, B. Williams, T.L. Buckwalter, K.M. La Perle, G. Hinkle, R. Pozderac, R. Kloos, H.N. Nagaraja, R.F. Barth, S.M. Jhiang, *Gene Ther.* 9 (2002) 1139–1145.
- [10] D. Dingli, R.M. Diaz, E.R. Bergert, M.K. O'Connor, J.C. Morris, S.J. Russell, *Blood* 20 (2003) 20.
- [11] J.W. Smit, J.P. Schroder-van der Elst, M. Karperien, I. Que, M. Stokkel, D. van der Heide, J.A. Romijn, *J. Clin. Endocrinol. Metab.* 87 (2002) 1247–1253.
- [12] U. Haberkorn, R. Kinscherf, M. Kissel, W. Kubler, M. Mahmut, S. Sieger, M. Eisenhut, P. Peschke, A. Altmann, *Gene Ther.* 10 (2003) 774–780.
- [13] U. Haberkorn, P. Beuter, W. Kubler, H. Eskerski, M. Eisenhut, R. Kinscherf, S. Zitzmann, L.G. Strauss, A. Dimitrakopoulou-Strauss, A. Altmann, *J. Nucl. Med.* 45 (2004) 827–833.
- [14] A. Yoshida, S. Taniguchi, I. Hisatome, I.E. Royaux, E.D. Green, L.D. Kohn, K. Suzuki, *J. Clin. Endocrinol. Metab.* 87 (2002) 3356–3361.
- [15] A.M. Rodriguez, B. Perron, L. Lacroix, B. Caillou, G. Leblanc, M. Schlumberger, J.M. Bidart, T. Pourcher, *J. Clin. Endocrinol. Metab.* 87 (2002) 3500–3503.
- [16] J. Takamatsu, T. Hosoya, M. Tsuji, M. Yamada, Y. Murakami, S. Sakane, K. Kuma, N. Ohsawa, *Thyroid* 2 (1992) 193–196.
- [17] B. Czarnocka, D. Pastuszko, M. Janota-Bzowski, A.P. Weetman, P.F. Watson, E.H. Kemp, R.S. McIntosh, M.S. Asghar, B. Jarzab, E. Gubala, J. Wloch, D. Lange, *Br. J. Cancer* 85 (2001) 875–880.
- [18] R.B. Mandell, L.Z. Mandell, C.J. Link Jr., *Cancer Res.* 59 (1999) 661–668.
- [19] U. Haberkorn, M. Henze, A. Altmann, S. Jiang, I. Morr, M. Mahmut, P. Peschke, W. Kubler, J. Debus, M. Eisenhut, *J. Nucl. Med.* 42 (2001) 317–325.
- [20] B.B. Luzzio, C.B. Luzzio, E.G. Bamberger, A.S. Feliu, *Proc. Soc. Exp. Biol. Med.* 166 (1981) 546–550.
- [21] B. Drewinko, W. Mars, J. Minowada, K.H. Burk, J.M. Trujillo, *Cancer* 54 (1984) 1883–1892.
- [22] S.J. Weiss, N.J. Philp, E.F. Grollman, *Endocrinology* 114 (1984) 1090–1098.
- [23] H.Y. Yeang, F. Yusof, L. Abdullah, *Anal. Biochem.* 226 (1995) 35–43.
- [24] Y. Nakamoto, T. Saga, T. Misaki, H. Kobayashi, N. Sato, T. Ishimori, S. Kosugi, H. Sakahara, J. Konishi, *J. Nucl. Med.* 41 (2000) 1898–1904.
- [25] D. Dingli, K.W. Peng, M.E. Harvey, M.K. O'Connor, R. Cattaneo, J.C. Morris, S.J. Russell, *Blood* 103 (2004) 1641–1646.
- [26] S. Eskandari, D.D. Loo, G. Dai, O. Levy, E.M. Wright, N. Carrasco, *J. Biol. Chem.* 272 (1997) 27230–27238.
- [27] J. Van Sande, C. Massart, R. Beauwens, A. Schoutens, S. Costagliola, J.E. Dumont, J. Wolff, *Endocrinology* 144 (2003) 247–252.
- [28] C. Spitzweg, A.B. Dietz, M.K. O'Connor, E.R. Bergert, D.J. Tindall, C.Y. Young, J.C. Morris, *Gene Ther.* 8 (2001) 1524–1531.
- [29] T. Groot-Wassink, E.O. Aboagye, M. Glaser, N.R. Lemoine, G. Vassaux, *Hum. Gene Ther.* 13 (2002) 1723–1735.
- [30] T. Petrich, H.J. Helmeke, G.J. Meyer, W.H. Knapp, E. Potter, *Eur. J. Nucl. Med. Mol. Imaging* 29 (2002) 842–854.
- [31] D.J. Simpkin, T.R. Mackie, *Med. Phys.* 17 (1990) 179–186.
- [32] M. Huang, R.K. Batra, T. Kogai, Y.Q. Lin, J.M. Hershman, A. Lichtenstein, S. Sharma, L.X. Zhu, G.A. Brent, S.M. Dubinett, *Cancer Gene Ther.* 8 (2001) 612–618.